International Scholarly Research Network
ISRN Materials Science
Volume 2012, Article ID 623754, 15 pages
doi:10.5402/2012/623754

Research Article

Copper Corrosion Inhibition in 1 M HNO_3 by Two Benzimidazole Derivatives

P. M. Niamien,[1] H. A. Kouassi,[1] A. Trokourey,[1] F. K. Essy,[1] D. Sissouma,[2] and Y. Bokra[1]

[1] *Laboratoire de Chimie Physique, Université de Cocody-Abidjan, BP 582 Abidjan 22, Cote D'Ivoire*
[2] *Laboratoire de Chimie Organique Structurale, Université de Cocody-Abidjan, BP 582 Abidjan 22, Cote D'Ivoire*

Correspondence should be addressed to P. M. Niamien, niamienfr@yahoo.fr

Received 25 November 2011; Accepted 5 January 2012

Academic Editors: F. Cabrera-Escribano and Y. Sun

Corrosion behavior of copper in 1 M nitric acid containing either 2-mercaptobenzimidazole (MBI) or 2-thiomethylbenzimidazole (TMBI) was investigated experimentally and theoretically via weight loss method and quantum chemical approaches. It was found that the two compounds exhibit a very good performance as inhibitors for copper corrosion in the studied medium. Results show that the inhibition efficiencies increase with increasing temperature and increasing concentration of the inhibitors. It has been found that the studied compounds adsorb onto copper according to the modified Langmuir adsorption isotherm and the kinetic/thermodynamic isotherm of El-Awady. The thermodynamic adsorption parameters and kinetic corrosion parameters were determined and analyzed; on the bases of these parameters both physisorption and chemisorption were suggested for the studied compounds. Furthermore, the quantum chemical properties/descriptors most relevant to their potential action as corrosion inhibitors have been calculated. They include E_{HOMO}, E_{LUMO}, energy gap (ΔE), dipole moment (μ), hardness (η), softness (σ), the fractions of electrons transferred (ΔN), electrophilicity index (ω), and the total energy change (ΔE_T). The theoretical results were found to be consistent with the experimental data reported.

1. Introduction

Because of its excellent conductivity, good mechanical workability, and relatively low cost and reactivity, copper is one of the most important materials used widely in different industries, especially in central heating installations, car industry, energetic, oil refineries, sugar factories, marine environment, to name only a few of its various applications. Scale and corrosion products produced during the work of systems have some negative effects on their heat-exchange performance. Thus, acid washing is periodically carried out to descale and clean these systems. Acidic solutions are widely used in various industries for the cleaning of copper. The behavior of copper in acidic media is extensively investigated, and several ideas have been presented for the dissolution process [1, 2]. To avoid the base metal attack and to ensure the removal of corrosion products/scales alone, inhibitors are extensively used. Corrosion inhibitors are substances that protect metals against corrosion by decreasing the rate of corrosion processes. Many efficient inhibitors are heterocyclic organic compounds consisting of a π-system and/or O, N, P, or S heteroatoms [3–5]. Among them, azoles, benzotriazole, and its derivatives are the most often used organic inhibitors against copper corrosion. Unfortunately, it is proven that benzotriazole and its derivatives are highly toxic compounds; their use is limited therefore by the restrictions due to the protection of the environment [6]. Benzimidazole derivatives are well known because of their nontoxicity and good inhibitor effectiveness in various media [7, 8].

The efficiency of an organic compound as a successful inhibitor is mainly dependent on its ability to be adsorbed on the metal surface, which consists of the replacement of water molecule at a corroding interface. The adsorption of these compounds is influenced by the electronic structure of the inhibiting molecules [9, 10] and also by the steric factors, aromaticity, electron density at the donor atoms, and the presence of functional groups [11–14].

Adsorption can be described by two mean types of interactions [15].

Physisorption. It involves electrostatic forces between ionic charges or dipoles on the adsorbed species and the electric

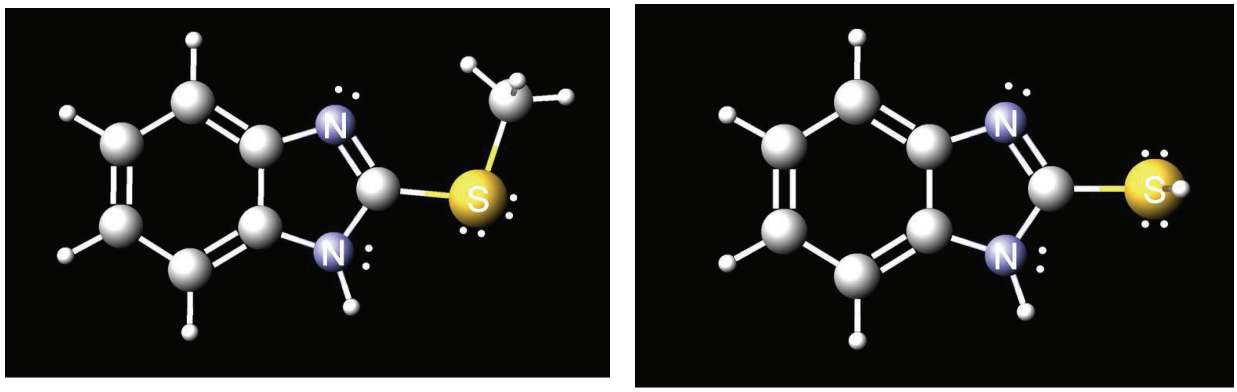

TMBI (a) MBI (b)

Figure 1: Optimized chemical structures of 2-thiomethylbenzimidazole (TMBI) and 2-mercaptobenzimidazole (MBI).

charge at the metal/solution interface. The heat of adsorption is low, and therefore this type of adsorption is stable only at relatively low temperatures.

Chemisorption. It involves charge sharing or charge transfer from the inhibitor molecule to the metal surface to form a coordinate type bond. In fact, electron transfer is typically for transition metals having vacant low-energy electron orbital. Chemisorption is typified by much stronger adsorption energy than physical adsorption. Such a bond is therefore more stable at higher temperature.

Thermodynamic adsorption parameters and kinetic corrosion parameters are a useful tool for clarifying the adsorption behaviour of an inhibitor. The reactivity of organic inhibitors is mainly interpreted by adsorption on the metal surface and depends on the molecular structure. In other words, the electronic structure of the organic compounds has a key influence on their corrosion inhibition efficiency. The molecular structure, including the electronic parameters, can be obtained by means of theoretical calculations by using the computational methodologies of quantum chemistry. Quantum chemical calculation has been used recently to explain the mechanism of corrosion inhibition [16–18] and proved to be a very powerful tool for studying the mechanism [19–21]. The survey of theoretical corrosion literature presented by Gece [19] demonstrates that quantum chemistry is a powerful tool to study the fundamental, molecular-level processes related to corrosion inhibition.The object of this paper is

(i) to evaluate the thermodynamic adsorption and the activation parameters of the copper/inhibitor/1 M HNO_3 system in the case of each of the selected compound. The choice of these compounds is based on molecular structure considerations; that is, these molecules are organic compounds having the same adsorption centers, but they only differ in the substituent CH_3 on *S* in TMBI.

(ii) To correlate the effect of structure parameters of the two compounds through their quantum parameters (E_{HOMO}, E_{LUMO}, $\Delta E = E_{HOMO} - E_{HOMO}$, μ, η, σ, ω) to explain their inhibition efficiency.

2. Materials and Methods

2.1. Molecules Structures. Figure 1 gives the structures of 2-mercaptobenzimidazole (MBI) and 2-thiomethylbenzimidazole (TMBI). Their molecular weight is respectively M = 150.2 g/moL and M = 164, 04 g/moL. These organic compounds have been synthesized in the Laboratory according to Van Allan method [22]. Their molecular structures have been identified by RMN-^{1}H and ^{13}C spectroscopies and mass spectroscopy.

MBI. RMN ^{1}H (DMSOd-6): 7.10–7.16 (2H,m), 7.22–7.34 (2H,m); ^{13}C NMR (DMSOd-6): 114.08 (2C) 121.39 (2C), 128.44 (2C), 149.66 (C=N); SDM (E.I.): M^{+1} = 151. Analysis for $C_7H_6N_2S$: C (55.97%), H (4.03%), N (18.65%), S (21.35%).

TMBI. RMN ^{1}H (acetone): 2.88 (s, 3H, $C\underline{H}_3$); 7.26–7.65 (2 m, 4H, $C_6\underline{H}_4$); RMN ^{13}C: 13.969 ($\underline{C}H_3S$); 115–121.4 (C_6H_4); 151.4 ($\underline{C}$=N); SDM (E.I.): M^{+1} = 165. Analysis for $C_8H_8N_2S$: C(58.51%), H(4.91%), N(17.06%), S(19.53%).

2.2. Weight-Loss Measurements. The weight loss method of monitoring corrosion rate is useful because of its simple application and reliability [23]. Several authors have reported on comparable agreement between weight-loss technique and other techniques of corrosion monitoring, including polarization measurement [24, 25], hydrogen evolution [26, 27], thermometric technique [28], and electrochemical impedance spectroscopy [29, 30].

The weight-loss measurements were performed with samples of copper in the form of rods measuring 10 mm in length and 2.2 mm in diameter that were cut from

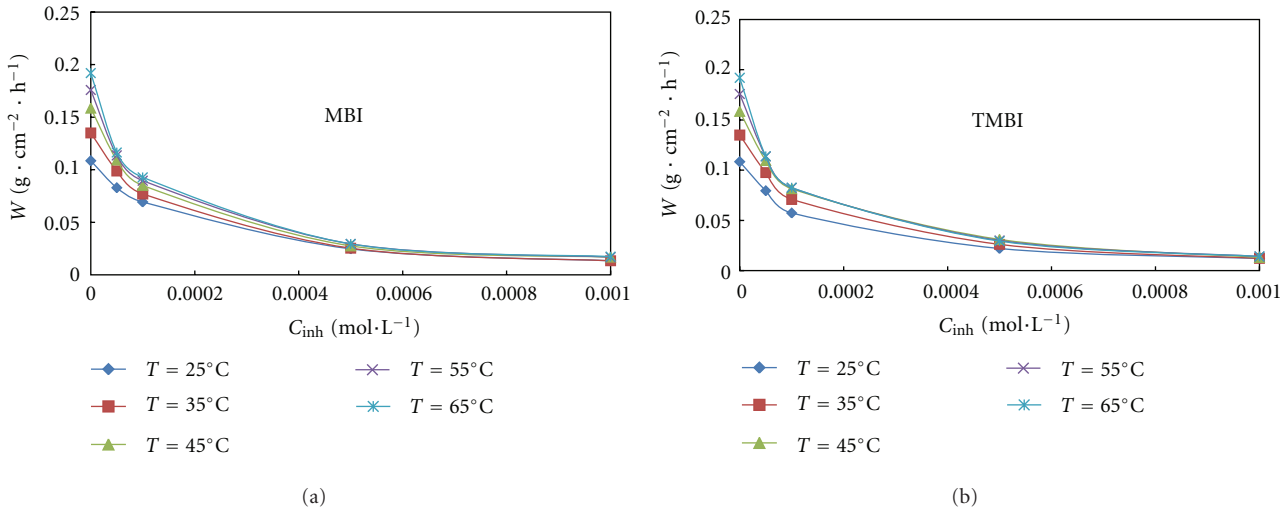

Figure 2: Dependence of copper corrosion rate on the inhibitors concentration at different temperatures. (a): MBI (b): TMBI.

commercial pure copper (Cu 99.5%). The corrosive solution of 1 M HNO_3 was prepared by dilution of analytical grade 65% HNO_3 from MERCK with double-distilled water. The samples were polished successively with metallographic emery papers of increasing fineness of up to 600 grits and further with 5, 1, 0.5, and 0.3 μm alumina slurries (Buehler), washed thoroughly with double-distilled water, degreased, and dried with acetone. The samples were then kept in a desiccator, weighed and immersed in the corrosive medium (50 mL of 1 M HNO_3) with or without the tested compounds. A water thermostat Selecta (Frigiterm) controlled to ±0.5°C maintained the temperatures ranging from 25°C to 65°C. After 1 hour, the specimens were removed, washed with double-distilled water, dried, kept in a desiccators, and then reweighed. All tests were made in aerated solutions and were run triplicate to guarantee the reliability of the results. The corrosion rate (W) was calculated using the following:

$$W = \frac{m_1 - m_2}{St}, \tag{1}$$

where m_1 and m_2 are, respectively, the weight (in g) before and after immersion in the test solution, S the total surface of the sample (in cm^2), and t the immersion time (in h).

The inhibition efficiency IE(%) was then calculated using the following:

$$\text{IE}(\%) = \frac{W_0 - W}{W_0} * 100, \tag{2}$$

where W_0 and W are, respectively, the corrosion rates of copper in the absence and presence of the tested compounds.

3. Results and Discussion

3.1. Effect of the Concentration of the Inhibitors on Corrosion Rate of Copper. Figures 2(a) and 2(b) represent the corrosion rate as a function of inhibitors concentration at different temperatures. It is clear that, for all temperature, corrosion rate decreases with increasing concentration. In other words, the addition of the molecules to 1 M HNO_3 solution retards copper corrosion, and the extend of retardation is concentration and temperature dependent. Similar observations have been seen in the literature [31]. However, we note that, for a given concentration, the corrosion rate increases with increasing temperature. This can be attributed to the fact that the rate of chemical reaction increases with increase in temperature.

3.2. Effect of the Inhibitors Concentration on the Inhibiting Efficiency. Figures 3(a) and 3(b) show the evolution of the inhibiting efficiencies with inhibitors concentration at different temperatures. Inspections of these figures reveal that inhibition efficiency increases with increasing concentration of each inhibitor. We also note that inhibition efficiency increases with increasing temperature. Such behavior can be interpreted on the basis that the inhibitors exert their action by adsorbing themselves on the metal surface and that the increase in temperature leads to a shift of the equilibrium constant towards adsorption of the inhibitors molecules. For a certain inhibitor concentration, the inhibitive action of the studied compounds can be given in the following increasing order: MBI < TMBI. Figure 4 gives the example of $C = 10^{-3}$ M. The ability of the molecule to adsorb on copper surface is probably dependent on the substituent on the sulfur atom. This result can be explained by orbital approach [32].

3.3. Activation Parameters. Arrhenius suggested the famous equation which evaluates the temperature dependence of the rate constant as follows [33]:

$$\log W = \log A - \frac{E_a}{2.303\ RT}. \tag{3}$$

Here, A is the frequency factor (in $g \cdot cm^{-2} \cdot h^{-1}$), E_a is the apparent activation energy (in $J \cdot mol^{-1}$), R is the perfect gas constant ($R = 8.314\ J \cdot moL^{-1} \cdot K^{-1}$), and T is the absolute

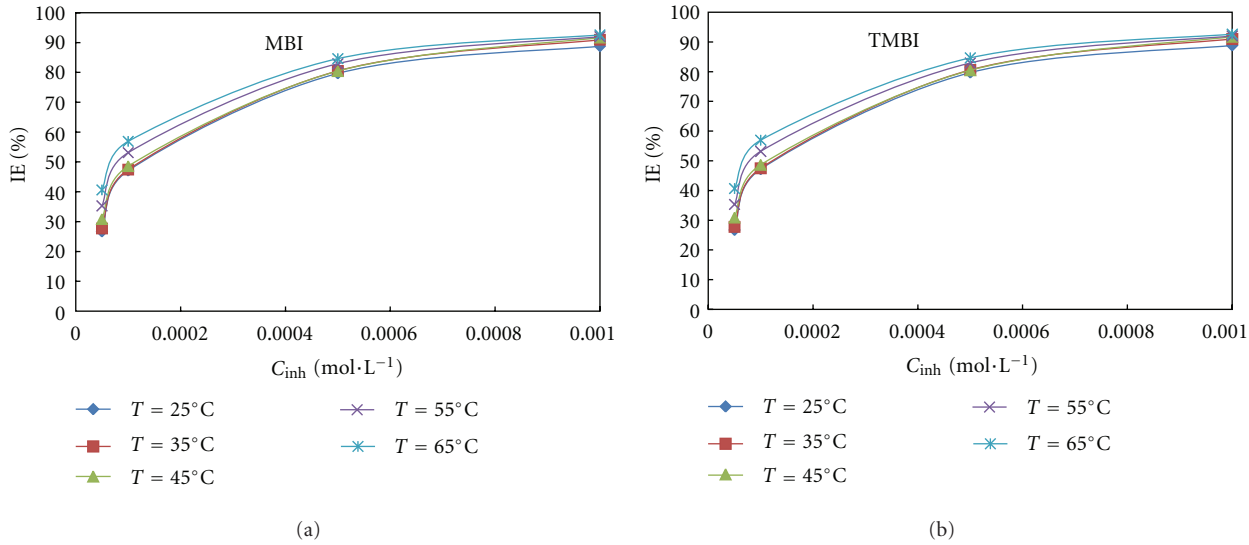

Figure 3: Variation of inhibition efficiency with inhibitors concentration for copper corrosion inhibition by (a): MBI (b): TMBI.

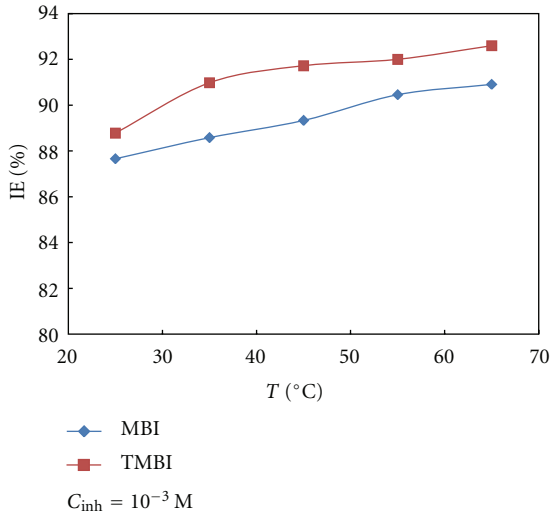

Figure 4: Evolution of the inhibiting efficiency of the studied compounds with the temperature for copper corrosion inhibition in 1 M HNO_3.

temperature (in K). Equation (3) predicts that the plot of log W versus $1/T$ should be a straight line. The slope of the line is ($-E_a$/2.303R), and the intercept of the line extrapolated ($1/T$ = 0) gives log A.

On the other hand, activation thermodynamic parameters including change in enthalpy (ΔH_a^*), change in free energy (ΔG_a^*), and change in entropy (ΔS_a^*) of activation were calculated using the following [34]:

$$\Delta H_a^* = E_a - RT,$$
$$\Delta G_a^* = 2.303\,RT\left[\log\left(\frac{k_B T}{h}\right) - \log W\right] \quad (4)$$
$$\Delta S_a^* = \left(\frac{\Delta H_a^* - \Delta G_a^*}{T}\right),$$

where K_B is the Boltzmann constant ($1.38\cdot10^{-23}$J·K^{-1}), h is the Planck constant ($6.626\cdot10^{-34}$ J·s), and R is the perfect gas constant. Figure 5 gives the representation of log W versus $1/T$.

All the activation thermodynamic parameters (E_a, ΔH_a^*, ΔS_a^*, and ΔG_a^*) are estimated and listed in Table 1.

From Table 1 it can be seen that, in general, values of the apparent activation energy E_a for the inhibited solutions are lower than that for the uninhibited one, indicating a chemisorption process of adsorption [35]. The energetic barrier is lower, facilitating the formation of Cu^{2+} ions which interact with the studied inhibitors to form a protective film [36]. Indeed it is proven that copper is corroded in Cu^{2+} in HNO_3 solution, and no oxide film is formed to protect the surface from corrosion [37, 38]. So in HNO_3 solution the following reactions occur:

$$Cu_2O + 2H^+ \rightleftarrows 2\,Cu^+ + H_2O$$
$$CuO + 2H^+ \rightleftarrows Cu^{2+} + H_2O \quad (5)$$

Moreover, Cu^+ ions undergo disproportionation according to the equation below:

$$2Cu^+ \rightleftarrows Cu^{2+} + Cu \quad (6)$$

The average values of apparent activation energies for MBI and TMBI are, respectively, 6.18 and 7.78 kJ·moL^{-1}. According to these values one can give the inhibitive character of the studied compounds in the following order: TMBI > MBI.

The positive sign of the activation enthalpy reflects the endothermic nature of copper dissolution process meaning that the dissolution of copper is difficult.

The negative values of ΔS_a^* in the inhibited and uninhibited systems impliy that activation complex in the rate-determining step represents an association rather than a dissociation step, meaning that a decrease disorder takes place on going from reactants to the activated complex [39].

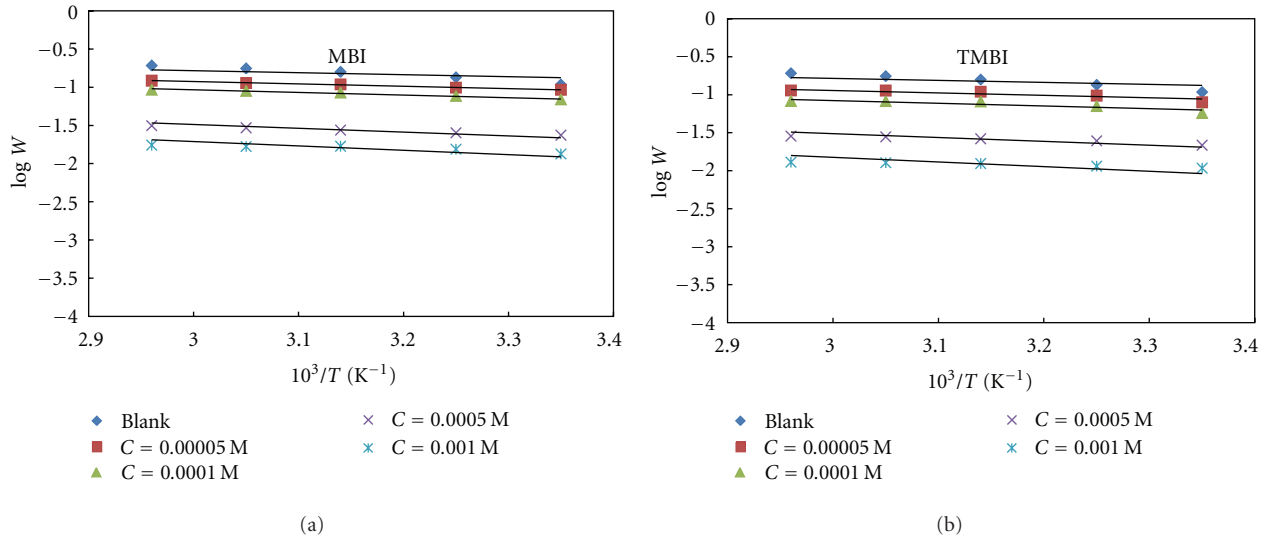

Figure 5: Arrhenius plots for copper corrosion in 1 M HNO_3 (a): MBI (b): TMBI.

Table 1: Corrosion kinetic parameters for copper in 1 M HNO_3 in absence and presence of the investigated inhibitors.

Concentration (M)	E_a (kJ·mol^{-1})	ΔH_a^* (kJ·mol^{-1})	ΔS_a^* (J·mol^{-1}·K^{-1})	ΔG_a^* (kJ·mol^{-1})
Blank				
0	12.24	9.60	−233.3	83.85
MBI				
$5\cdot10^{-5}$	6.49	3.85	−251.5	83.82
10^{-4}	6.29	3.65	−254.1	84.45
$5\cdot10^{-4}$	6.14	3.49	−263.7	87.36
10^{-3}	5.79	3.15	−269.2	88.77
TMBI				
$5\cdot10^{-5}$	9.85	7.21	−241.0	83.86
10^{-4}	9.48	6.84	−244.8	84.70
$5\cdot10^{-4}$	6.88	4.24	−261.3	87.32
10^{-3}	4.92	2.27	−273.6	89.28

3.4. Thermodynamic Adsorption Parameters. Since the corrosion inhibition process is based on the adsorption of the inhibitor molecules on the metal surface, it is essential to know the mode of adsorption and the adsorption isotherm that fits the experimental results. The values of surface coverage for various concentrations of the inhibitors under investigation must be used to explain the best adsorption isotherm. It is a widely held view by many authors that the adsorption of organic inhibitor molecules on metal surface is often a displacement reaction involving the removal of adsorbed water molecules from this surface [40, 41]

$$\mathrm{Org}_{\mathrm{sol}} + n\mathrm{H_2O}_{\mathrm{ads}} \longleftrightarrow \mathrm{Org}_{\mathrm{ads}} + n\mathrm{H_2O}_{\mathrm{sol}} \quad (7)$$

The surface coverage (θ) was calculated as follows:

$$\theta = \frac{\mathrm{IE}(\%)}{100}. \quad (8)$$

Basic information on the interaction between the inhibitor and the copper surface can be provided by the adsorption isotherm. It is necessary to determine empirically which adsorption isotherm fits best to the surface coverage data in order to use the corrosion rate measurements to calculate the thermodynamic parameters pertaining inhibitor adsorption. In order to obtain the isotherm, linear relation between θ values and the inhibitor concentration C must be found. Attempts were made to fit the θ values to various isotherms including Langmuir, Temkin, Frumkin, Freundlich, and the kinetic/thermodynamic isotherm of El-Awady. The best fit was obtained with the Langmuir isotherm and that of El-Awady.

The Langmuir adsorption isotherm is described by the following:

$$\frac{C}{\theta} = \frac{1}{K} + C, \quad (9)$$

where C is the inhibitor concentration, θ is the fraction of the surface covered, and K the equilibrium constant of the adsorption process. Figure 6 shows the dependence of C/θ as

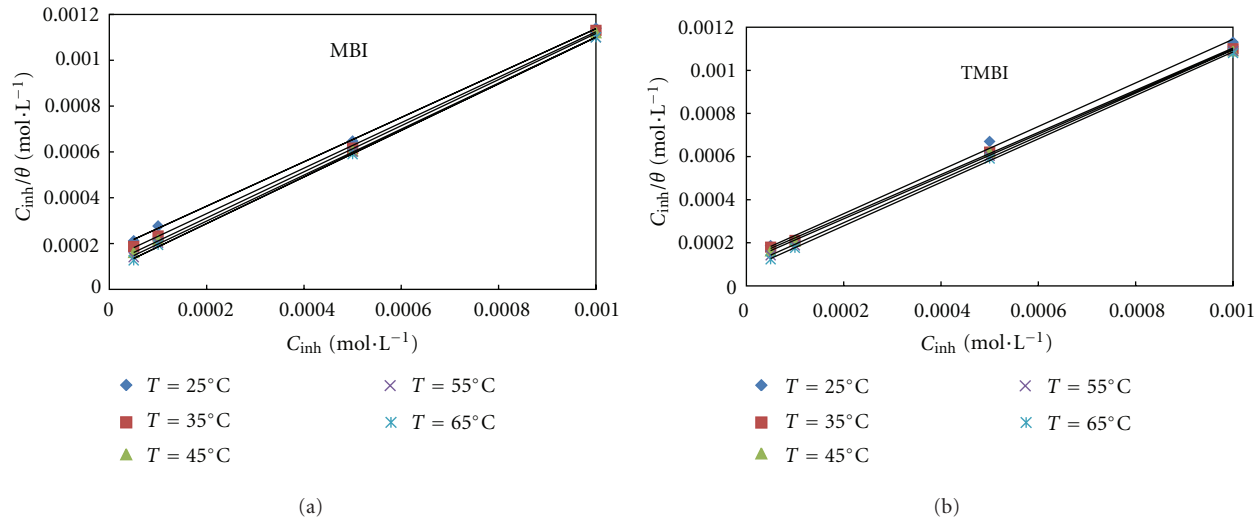

Figure 6: Langmuir adsorption isotherm for the investigated inhibitors at different temperatures.

Table 2: Calculated parameters from modified Langmuir isotherm and El-Awady adsorption isotherm at $C = 10^{-3}$ M.

Inhibitor	Temperature T(K)	Modified Langmuir isotherm				El-Awady isotherm			
		K_{ads} (10^5 M^{-1})	ΔG°_{ads} (kJ·mol^{-1})	Slope	R^2	K_{ads} (10^5 M^{-1})	ΔG°_{ads} (kJ·mol^{-1})	$1/y$	R^2
MBI	298	0.71	−31.93	0.968	0.999	0.63	−31.63	0.941	0.998
	308	0.77	−33.19	0.992	0.999	0.71	−32.98	0.957	0.997
	318	0.83	−34.48	1.005	0.999	0.85	−34.52	1.006	0.998
	328	1.00	−36.06	1.004	0.999	0.91	−35.80	0.982	0.973
	338	1.01	−37.16	1.016	0.999	1.16	−37.58	1.067	0.996
TMBI	298	0.80	−32.18	1.007	0.999	0.84	−32.33	1.029	0.984
	308	0.96	−33.88	0.977	0.999	0.90	−33.58	0.949	0.994
	318	1.11	−35.23	0.982	0.999	1.02	−35.00	0.964	0.990
	328	1.15	−36.44	0.998	0.999	1.19	−36.55	1.009	0.995
	338	1.25	−37.49	1.008	0.999	2.96	−40.20	1.051	0.996

a function of the concentration C for MBI and TMBI. The obtained plots are linear with correlation coefficients (R^2) almost equal to unity. It is also found that all the values of the slopes are very close to unity (Table 2). The deviation of the slopes from unity is often interpreted as a sign that the adsorption species occupy more or less a typical adsorption site at the metal/solution interface [42]. The divergence of the slopes from unity is attributable to interactions between adsorbate species on the metal surface as well as changes in the adsorption heat with increasing surface coverage. The Langmuir adsorption isotherm cannot be applied rigorously. A modified Langmuir adsorption isotherm [43] can be applied to this phenomenon which is given by the corrected

$$\frac{C}{\theta} = \frac{n}{K_{ads}} + nC. \tag{10}$$

The equilibrium constant of adsorption is related to the standard free energy of adsorption ΔG^0_{ads} by the following:

$$K_{ads} = \frac{1}{55.5} \cdot \exp\left(-\frac{\Delta G^0_{ads}}{R.T}\right), \tag{11}$$

where R is universal gas constant, T is the absolute temperature, and 55.5 is the molar concentration of water in the solution in mol·L^{-1}. The adsorption equilibrium constant and the standard free energy of adsorption ΔG^0_{ads} (Table 2) were calculated for $C = 10^{-3}$ M, using (10) and (11).

The experimental data were also well described by the El-Awady kinetic/thermodynamic adsorption isotherm. The characteristic equation of this model is given by

$$\log\left(\frac{\theta}{1-\theta}\right) = \log K + y \log C, \tag{12}$$

where C is the concentration of the inhibitors, θ is the degree of surface coverage, K_{ads} is the equilibrium constant

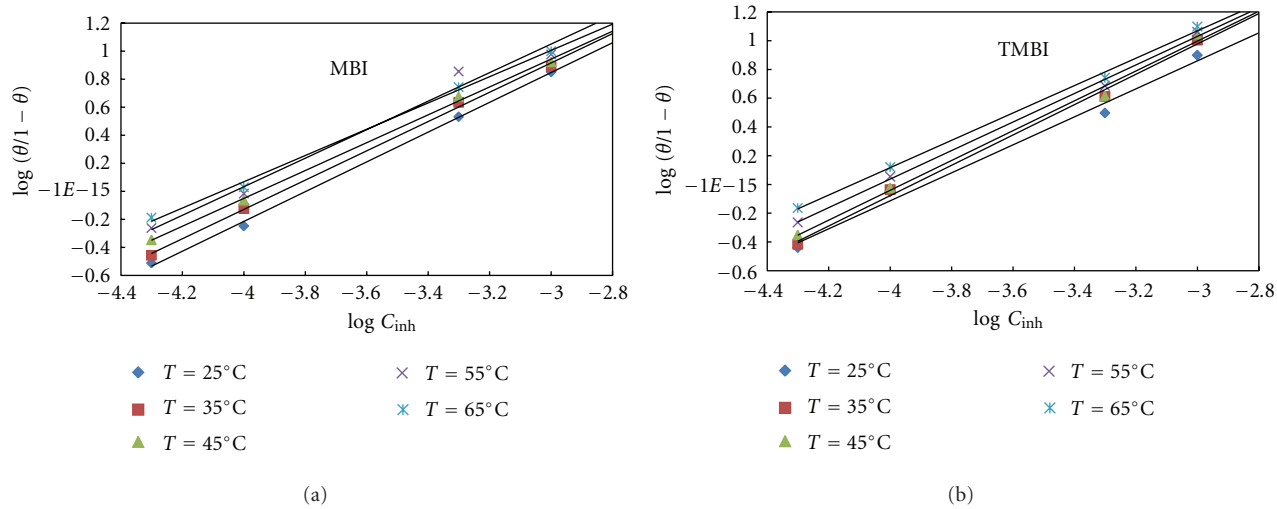

Figure 7: El-Awady adsorption isotherm for the investigated inhibitors at different temperatures.

of the adsorption process, and $K_{ads} = K^{1/y}$. In this model, the number of active sites y is included. Values of $1/y$ less than one imply multilayer adsorption, while $1/y$ greater than one suggests that a giving inhibitor molecule occupies more than one active site. Curve fitting of the data to the thermodynamic/kinetic model is shown in Figure 7. These plots give straight lines which clearly show that the data fit well to the isotherm. The values of K_{ads} and ΔG^0_{ads} for $C = 10^{-3}$ M are listed in Table 2. From the table, it can be seen that values of $1/y$ are very closed to the unity.

The negative values of ΔG^0_{ads} indicate a spontaneous adsorption process of MBI and TMBI on copper [44]. It is generally accepted that, for the values of ΔG^0_{ads} up to -20 kJ/moL, the type of adsorption was regarded as physisorption; the inhibition acts due to the electrostatic interactions between the charged molecules and the charged metallic surfaces, while the values around -40 kJ/moL or smaller were seen as chemisorption, which is due to the charge sharing or a transfer from the inhibitors molecules to the metal surface to form a covalent bond [45, 46]. The values of ΔG^0_{ads} in our measurements range from -30 to $-40\,\text{kJ}\cdot\text{moL}^{-1}$. it is suggested that the adsorption of these molecules involves both types of interactions, chemisorptions, and physisorption.

ΔG^0_{ads} is related to the enthalpy change and entropy change of adsorption process, ΔH^0_{ads} and ΔS^0_{ads}, respectively by Gibbs equation

$$\Delta G^0_{ads} = \Delta H^0_{ads} - T\Delta S^0_{ads}. \quad (13)$$

Using the obtained values of ΔG^0_{ads} from the modified Langmuir isotherm, we can plot ΔG^0_{ads} versus T (Figure 8). These plots give straight lines with slopes $(-\Delta S^0_{ads})$ and intercepts (ΔH^0_{ads}). The obtained values of the lines parameters are listed in Table 3.

The values of thermodynamic parameters for the adsorption of the tested molecules can provide valuable information about the mechanism of corrosion inhibition. The endothermic adsorption process ($\Delta H^0_{ads} > 0$) is attributed unequivocally to chemisorption [47], while generally, an exothermic adsorption process ($\Delta H^0_{ads} < 0$) may involve either physisorption or chemisorption or a mixture of both the processes. In the present case, the positive values of ΔH^0_{ads} indicate that the adsorption of the tested compounds is an endothermic process. The positive values of ΔS^0_{ads} indicate that the adsorption of these molecules is a process accompanied by an increase in entropy change, favoring the adsorption of the molecules onto the surface of the metal.

3.5. Mechanism of Inhibition. As far as the inhibition process is concerned, it is generally assumed that adsorption of an organic inhibitor at the metal/solution interface is the first step in the action mechanism of the organic compounds in aggressive acidic media. Four types of adsorption may take place during inhibition involving organic molecules at the metal/solution interface:

(i) electrostatic attraction between charged molecules and the charged metal,

(ii) interaction of unshared electron pairs in the molecule with the metal,

(iii) interaction of π-electrons with the metal,

(iv) a combination of the above situations [48].

Concerning inhibitors, the inhibition efficiency depends on several factors, such as the number of adsorption sites and their charge density, molecular size, heat of hydrogenation, mode of interaction with the metal surface, and the formation metallic complexes [49].

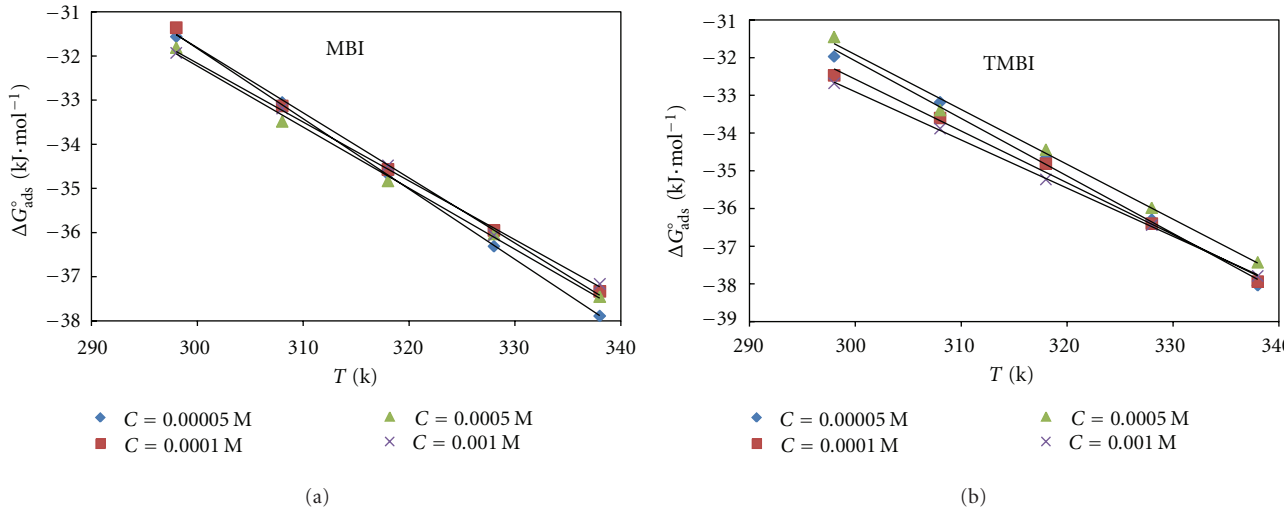

Figure 8: Gibbs plots for copper corrosion in 1 M HNO_3 at different concentrations (a): MBI (b): TMBI.

Table 3: Gibbs plots parameters for copper corrosion in 1 M HNO3 for different concentrations.

Inhibitor C (M)	ΔH^0_{ads} (kJ·mol^{-1})	ΔS^0_{ads} (J·mol^{-1}·K^{-1})	R^2
MBI			
$5\cdot10^{-5}$	15.93	159.2	0.999
10^{-4}	12.47	147.6	0.996
$5\cdot10^{-4}$	9.26	138.3	0.996
10^{-3}	7.82	133.3	0.997
TMBI			
$5\cdot10^{-5}$	13.70	152.6	0.994
10^{-4}	12.05	147.4	0.992
$5\cdot10^{-4}$	11.53	145.5	0.991
10^{-3}	8.72	137.8	0.995

In our case, the two molecules (MBI and TMBI) can be protonated in HNO_3 solution. Thus, they become cations, existing in equilibrium with the corresponding molecular form [50–52]

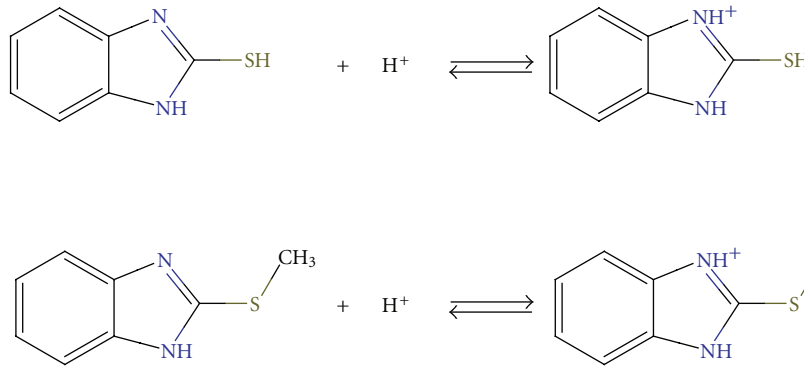

(14)

On the other hand, in 1 M HNO_3, copper is corroded in Cu^{2+}, and the surface of copper is positively charged. NO_3^- ions are attracted by the charges on the copper surface which tends to be charged negatively.

The obtained results could be explained on the assumption that the negatively charged NO_3^- would attach to the positively charged surface. There may be a synergism between NO_3^- and the protonated inhibitors $[MBIH]^+$ and

$[TMBIH]^+$ near the interface, and the concentrations of NO_3^- and that of the neutral forms (MBI and TMBI) and the protonated forms of the inhibitors ($[MBIH]^+$ and $[TMBIH]^+$) were probably much higher than those in the bulk solution; the protonated forms did attach electrostatically to the negative charges at the copper surface. When the neutral forms and the protonated forms of the inhibitors adsorb on the copper surface, coordinate bonds are formed by partial transference of electrons from the unprotonated N atoms, sulfur atoms, delocalized π electrons in the benzimidazole rings to the metal surface via vacant d orbitals of Cu^{2+} ions. So, in the process of adsorption, both physical and chemical adsorptions might take place. Similar mechanism has been proposed by Tang et al. [53]. The inhibitory mechanism on copper dissolution is related to the chelating effect of Cu^{2+} ions close to copper surface. Indeed, it is proven that copper is corroded to Cu^{2+} in HNO_3 solution and no oxide film is formed to protect the surface from corrosion [37, 38]. It is also known that the organic compounds can be adsorbed by the interactions between the lone pairs of electrons of nitrogen, sulfur, or oxygen atoms with metal surface. These processes are facilitated by the presence of d vacant orbitals of low energy in the copper ions, as observed in transition group metals. Recently, it was found that the formation of donor-acceptor surface complexes between free electrons of an inhibitor and a vacant d orbital of a metal is responsible for the inhibition corrosion process [54]. The number of Cu^{2+} ions in proximity of copper increases with increasing temperature, leading to the formation of Cu^{2+}-inhibitor complexes protective film (increase in surface coverage) which create a physical barrier between Cu surface and the electrolyte, retarding the dissolution of the metal [36]. The inhibition efficiency is then enhanced with increase in temperature.

3.6. Quantum Chemistry Studies

3.6.1. Theoretical Details. In order to support experimental data, theoretical calculations were conducted in order to provide molecular-level understanding of the observed experimental behavior. Among quantum chemical methods for evaluation of corrosion inhibitors, density functional theory, DFT has shown significant promise [55] and appears to be adequate for pointing out the changes in electronic structure responsible for inhibitory action.

There is no doubt that the recent progress in DFT has provided a very useful tool for understanding molecular properties and for describing the behavior of atoms in molecules. DFT methods have become very popular in the last decade due to their accuracy that is similar to other methods in less time and with a smaller investment from the computational point of view. In agreement with the DFT, the energy of the fundamental state of polyelectronic systems can be expressed through the total electronic density, and in fact the use of the electronic density instead of the wave function for the calculation of the energy constitutes the fundamental base of DFT [56]. Several quantum chemical methods and molecular modeling techniques have been performed to correlate the inhibition efficiency of the inhibitors with their molecular properties [16, 41, 57–63]. The reactive ability of the inhibitor is closely linked to their frontier molecular orbitals (FMOs), including highest occupied molecular orbital, HOMO, and lowest unoccupied molecular orbital, LUMO, and the other parameters such as hardness and softness, and so forth. Density functional theory (DFT) has become an attractive theoretical method because it gives exact basic vital parameters for even huge complex molecules at low cost [54, 64, 65]. Furthermore, by using sophisticated computational tools, we can understand reactivity behavior of hard and soft acid-base (HSAB) theory that provides a systematic way for the analysis of the inhibitor/surface interaction [66]. Thus, DFT has become a main source of connecting some traditional empirical concepts with quantum mechanics. Therefore, DFT is a very powerful technique to probe the inhibitor/surface interaction and to analyze experimental data.

For an N-electrons system with total electronic energy (E) and an external potential $V(r)$, chemical potential (μ_P), known as the negative of electronegativity (χ), has been defined as the first derivative of the total energy with respect to N at $V(r)$ [67]

$$\chi = -\mu_P = -\left(\frac{\partial E}{\partial N}\right)_{V(r)}. \tag{15}$$

Hardness (η) has been defined within the DFT theory as the second derivative of the total energy with respect to N at $V(r)$ property which measures both the stability and reactivity of a molecule [68]

$$\eta = \left(\frac{\partial^2 E}{\partial N^2}\right)_{V(r)} = \left(\frac{\partial \mu_P}{\partial N}\right)_{V(r)}. \tag{16}$$

In this formula, E is the electronic energy, N is the number of electrons, $V(r)$ is the external potential due to the nuclei, and μ_P is the chemical potential.

The number of electrons transferred (ΔN) from the inhibitor molecule to the metal surface can be calculated using the following [69]:

$$\Delta N = \frac{\chi_{\mathrm{Cu}} - \chi_{\mathrm{inh}}}{2\,(\eta_{\mathrm{Cu}} + \eta_{\mathrm{inh}})}, \tag{17}$$

where χ_{Cu} and χ_{inh} are the absolute electronegativity of copper and inhibitor molecule, respectively; η_{Cu} and η_{inh} are the absolute hardness of copper and the inhibitor molecule, respectively.

The ionization potential (I) and the electron affinity (A) are related to E_{HOMO} and E_{LUMO} by the following [70]:

$$\begin{aligned} I &= -E_{\mathrm{HOMO}}, \\ A &= -E_{\mathrm{LUMO}}. \end{aligned} \tag{18}$$

These quantities are related to the absolute electronegativity and the absolute hardness by the equations below [70]

$$\begin{aligned} \chi &= \frac{I + A}{2}, \\ \eta &= \frac{I - A}{2}. \end{aligned} \tag{19}$$

Global softness can also be defined as [71]

$$\sigma = \frac{1}{\eta} = \frac{2}{I - A}. \quad (20)$$

Actually, a new global chemical reactivity parameter has been introduced and is called electrophilicity index (ω). This parameter is defined as [72]

$$\omega = \frac{\mu_P^2}{2\eta} = \frac{\chi^2}{2\eta}. \quad (21)$$

This parameter measures the electrophilic power of a molecule.

Let's consider the situation corresponding to a molecule that is going to receive certain amount of charge at some center and is going to backdonate a certain amount of charge through the same center or another one. To describe the energy charge associated with these two processes, the hardness is fixed to the value of $\eta = (\mu_P{}^+ - \mu_P{}^-)$ in both situations. Thus, according to the simple charge transfer model for donation and backdonation of charges proposed recently [73], when a molecule receives a certain amount of charge ΔN^+ associated with the energy change ΔE^+

$$\Delta E^+ = \mu_P{}^+ \Delta N^+ + \frac{1}{2}\eta(\Delta N^+)^2. \quad (22)$$

When a molecule backdonates a certain amount of charge ΔN^- associated with the energy change ΔE^-, then

$$\Delta E^- = \mu_P{}^- \Delta N^- + \frac{1}{2}\eta(\Delta N^-)^2. \quad (23)$$

If the total energy change is approximated by the sum of the contributions of (22) and (23), and assuming that the amount of charge backdonation is equal to the amount of charge received: $\Delta N^- = -\Delta N^+$, then

$$\Delta E_T = \Delta E^+ + \Delta E^- = (\mu_P{}^+ - \mu_P{}^-)\Delta N^+ + \eta(\Delta N^+)^2. \quad (24)$$

The total energy change is minimum with respect to ΔN^+ and implies that $\Delta N^+ = -(\mu_P{}^+ + \mu_P{}^-)/2\eta$ and that

$$\Delta E_T = \frac{-(\mu_P{}^+ - \mu_P{}^-)^2}{4\eta} = -\frac{\eta}{4}. \quad (25)$$

3.6.2. Computational Details. The aim in this part of the work is to correlate the observed inhibition efficiency with the quantum chemical parameters of the investigated inhibitors. All the calculations were performed by resorting to density-functional theory (DFT) method using the Gaussian 03 W suite of programs. To establish correlation between experimental data and structural and electronic characteristics of the studied compounds, the geometry of the molecules (Figure 1) was optimized by the density functional theory (DFT) method level with B3LYP exchange correlation functional, using 6–31G (d, p) basis set. This basis set provided accurate geometry and electronic properties for a wide range of organic compounds [19, 74].

Table 4: The calculated quantum chemical parameters and descriptors for MBI and TMBI obtained using DFT at B3LYP/6–31(d, p) basis set.

Parameter	MBI	TMBI
E_{HUMO} (eV)	−6.033	−5.856
E_{LUMO} (eV)	−0.639	−0.556
$\Delta E = E_{LUMO} - E_{HUMO}$ (eV)	5.394	5.300
μ (D)	3.8428	1.7862
I (eV)	6.033	5.856
A (eV)	0.639	0.556
X (eV)	3.257	3.084
η (eV)	2.783	2.729
ΔN (e)	0.305	0.334
σ (eV^{-1})	0.359	0.366
ω (eV)	2.063	1.939
ΔE_T (eV)	−0.696	−0.682

3.6.3. Correlation between Molecular Orbital Energy Level and Inhibition Efficiency. According to the frontier molecular orbital theory, the chemical reactivity is a function of interaction between HOMO and LUMO levels of the reacting species [62]. E_{HOMO} is a quantum chemical parameter often associated with the electron donating ability of the molecule. High value of E_{HOMO} indicates a tendency of the molecule to donate electrons to appropriate acceptor system of low empty molecular orbital energy [20]. The energy of lowest unoccupied molecular orbital, E_{LUMO}, therefore, indicates the ability of the molecule to accept electrons [71]. So, the lower the value of E_{LUMO}, the more probable the molecule would accept electrons. Thus, the binding ability of the inhibitor to the metal surface increases with increasing of the HOMO and decreasing of the LUMO energy values.

Other indicators are absolute electronegativity (χ), absolute hardness (η), and absolute softness (σ). The absolute electronegativity is the chemical property that describes the ability of a molecule to attract electron towards itself in a covalent bond, while the absolute hardness is measured by the energy gap between the lowest unoccupied and the highest occupied molecular orbitals.

Let's consider two systems with different electronegativity as a metallic surface and an inhibitor molecule; the following mechanism will take place: the electron flow will happen from the system with the low electronegativity towards that of a higher value until the chemical potentials are the same.

In order to calculate the fraction of electrons transferred, a theoretical value of electronegativity of bulk copper was used $\chi_{Cu} = 4.98$ eV [75] and a global hardness assuming that for a metallic bulk $I = A$ [76] because they are softer than the neutral metallic atoms. All the calculated quantum chemical parameters are listed in Table 4.

From Table 4, it can be clearly seen that the values of E_{HOMO} are in descent order as TMBI > MBI. This is in agreement with the experimentally determined inhibition efficiencies (Figure 4). For E_{LUMO}, we have the same order

Table 5: Atomic charges with hydrogen summed into heavy atoms obtained using DFT at B3LYP/6–31(d, p) basis set.

Compound	–N=	–NH–	–S–
MBI	−0.538551	−0.295407	−0.066943
TMBI	−0.651433	−0.294465	−0.257838

TMBI > MBI which follows the order of the inhibition efficiencies. These results show that TMBI has more tendencies to bond with copper by donating electrons.

The energy gap $\Delta E = E_{\text{LUMO}} - E_{\text{HOMO}}$ is an important parameter, and it is a function of reactivity of the inhibitor molecule towards the adsorption on metallic surface. As ΔE decreases, the reactivity of the molecule increases, leading to increase in inhibition efficiency of the molecule [77]. The values of ΔE in Table 4 show the following relation: MBI > TMBI, which is in agreement with the inhibition efficiencies obtained for the inhibitors.

The bonding tendencies of the inhibitors towards copper can be discussed in terms of hard-soft-acid-base (HSAB) and the frontier controlled interaction concepts [78, 79]. General rule suggested by the principle of HSAB is that hard acids prefer to coordinate to hard bases, and soft acids prefer to coordinate to soft bases. On the other hand, metal atoms are known as soft acids. Hard molecules have high HOMO-LUMO gap, and soft molecule has a small HOMO-LUMO gap [80], and thus soft bases inhibitors are the most effective for metals [77]. In our case, TMBI, which has the lowest energy gap (ΔE) and the highest softness (σ), has the most inhibition efficiency [81]. We can observe from Table 4 that the values of the hardness (η) of the two molecules are in the following order: TMBI < MBI. This order is the reverse of that obtained for softness. So the inhibitor with the least value of global hardness (hence the highest value of global softness) is the best and vice versa. These results are consistent with the results obtained for experimental efficiencies.

In Table 4, we can also see the calculated values of the number of electrons transferred (ΔN). Values of this parameter show that the inhibition efficiency resulting from electron donation agrees with Lukovits's study [69]. If $\Delta N < 3.6$, the inhibition efficiency increases by increasing electron-donating ability of the inhibitors to the metal surface. The calculated values of ΔN correlate strongly with experimental inhibition efficiencies. Thus, the highest fraction of electrons transferred is associated with the best inhibitor (TMBI), while the least fraction is associated with the inhibitor that has the least inhibition efficiency (MBI).

The electrophilicity index (ω) expresses the ability of the inhibitor molecules to accept electrons; in our case, the values are nearly the same for the studied inhibitors (Table 4); the two inhibitors have nearly the same capacity to accept electrons. The unoccupied d orbitals of Cu^{2+} ($[Ar]3d^9$) can accept electrons from the inhibitors to form coordinate bond. On the other hand, the inhibitors molecules can accept electrons from Cu^{2+} ion with its antibonding orbitals to form backdonating bond. These donation and back donation processes strengthen the adsorption of the inhibitors molecules onto copper surface [16].

Signs of hardness ($\eta > 0$) and that of the total energy change ($\Delta E_T < 0$) (Table 4) show that the charge transfer to the molecule followed by backdonation from the molecule is energetically favorable (charge transfer to the molecule and backdonation from the molecule). Similar observation has been reported in the literature [73]. However, we must note that (25) does not predict that a back donation process is going to occur; it only establishes if both processes occur, the energy change is directly proportional to the hardness of the molecule.

The dipole moment (μ) is another parameter of the electronic distribution in a molecule and is the measure of polarity of a polar covalent bond. According to Khalil [82], lower values of dipole moments (μ) will favour accumulation of the inhibitor in the surface layer and therefore higher inhibition efficiency. In our case TMBI has the lower value of dipole moment and MBI the highest one. So considering Khalil's point of view, there is a good agreement between the experimental inhibition efficiency values and the obtained dipole moment values. According to Yurt and coworkers, in most cases, the adsorption power (IE (%) of the inhibitor) depends on certain physicochemical parameters (solubility, molecular size, etc.); it increases with lower dipole moments and with increasing nitrogen charge [46]. However, several authors state that the inhibition efficiency increases with increasing values of dipole moment [83, 84]. On the other hand, survey of the literature reveals that several irregularities appeared in case of correlation of dipole moment with inhibitor efficiency [85, 86]. So in general, there is no significant relationship between the dipole moment values and inhibition efficiencies [19].

3.6.4. Correlation between Atomic Charge and Inhibition Efficiency. Frontier orbital energy level indicates the tendency of bonding to the metal surface. Further study on the formation of chelating centers in an inhibitor requires the information of spatial distribution of electronic density of the molecule [87].

The structure of the molecule can affect the adsorption, influencing the electron density at the functional group. Generally, electrophile systems attack the molecule at negatives charged sites. It is proven that the electron density focused on heteroatoms (S, N, O, Se, P,...) which are the active centers [88]; these atoms have the strongest ability of bonding to the metal surface. We have listed in Table 5 the charges of polar atoms which are the centers of the studied compounds, which favor the adsorption of these molecules onto copper surface.

From Table 5, it can be seen that charges on nitrogen are nearly similar even if TMBI has the highest global partial charge and MBI the lowest one. We note that great differences exist between charges on S. The absolute values of these

partial charges are in descent order as $\delta_{S(TMBI)} > \delta_{S(MBI)}$. Inhibition efficiency and electronic charges on S atom have the same trend. The HOMO of TMBI and MBI is made up predominantly of 3_{px} of S atom in each molecule which contribute, respectively, to the electronic charge density of their HOMO levels. S atom of TMBI has the highest contribution, while that of MBI has the lowest one. This can be associated with the dominative contribution of the S atom according to the frontier orbital approximation; the region of highest density is generally the site of electrophilic attack [88].

N and S heteroatoms have lonely electron pairs that are important for bonding unfilled 3d orbitals of copper ion Cu^{2+}; they determine the adsorption of the molecules on the metal surface. TMBI has the highest inhibition efficiency, which result from the geometry change that led to HOMO energy increase and electron density distribution in the molecule. Based on the discussion above, it can be concluded that N and S atoms are the most possible sites of bonding metal surface by donating electrons to copper ions; the inhibition efficiency depends on the total charge (δ_T) on N and S of each molecule. On the other hand, the efficiency values of the two inhibitors can be explained by the fact that $-CH_3$ attached to benzimidazole ring (TMBI) has the ability to donate more electrons to the ring compared to $-H$ attached to benzimidazole ring (MBI).

4. Conclusion

From the present study, the main following conclusions can be drawn.

(1) The two compounds (TMBI and MBI) are good inhibitors for copper corrosion in 1 M HNO_3.

(2) Their inhibition efficiencies increase with increasing concentration and increasing temperature.

(3) The thermodynamic adsorption and activation parameters obtained support both physical and chemical adsorption mechanism.

(4) Adsorption of the two inhibitors on copper surface follows modified Langmuir adsorption model and the thermodynamic/kinetic adsorption model of El-Awady.

(5) The experimental results and the theoretical ones are in good agreement.

Acknowledgment

The authors acknowledge the financial support of the Laboratory of Physical Chemistry of University of Cocody-Abidjan (Côte d'Ivoire).

References

[1] G. Trabanelli, "Inhibitors—an old remedy for a new challenge," *Corrosion*, vol. 47, no. 6, pp. 410–419, 1991.

[2] A. Jardy, A. L. Lasalle-Molin, M. Keddam, and H. Takenouti, "Copper dissolution in acidic sulphate media studied by QCM and rrde under ac signal," *Electrochimica Acta*, vol. 37, no. 12, pp. 2195–2201, 1992.

[3] S. M. A. Hosseini and A. Azimi, "The inhibition of mild steel corrosion in acidic medium by 1-methyl-3-pyridin-2-yl-thiourea," *Corrosion Science*, vol. 51, no. 4, pp. 728–732, 2009.

[4] P. C. Okafor and Y. Zheng, "Synergistic inhibition behaviour of methylbenzyl quaternary imidazoline derivative and iodide ions on mild steel in H_2SO_4 solutions," *Corrosion Science*, vol. 51, no. 4, pp. 850–859, 2009.

[5] A. S. Fouda and A. S. Ellithy, "Inhibition effect of 4 phenylthiazole derivatives on corrosion of 304 L stainless steel in HCl solution," *Corrosion Science*, vol. 51, no. 4, pp. 868–875, 2009.

[6] H. Otmačić and E. Stupnišek-Lisac, "Copper corrosion inhibitors in near neutral media," *Electrochimica Acta*, vol. 48, no. 8, pp. 985–991, 2003.

[7] R. Gašparac, C. R. Martin, and E. Stupnišek-Lisac, "In situ studies of imidazole and its derivatives as copper corrosion inhibitors I. Activation energies and thermodynamics of adsorption," *Journal of the Electrochemical Society*, vol. 147, no. 2, pp. 548–551, 2000.

[8] D. Q. Zhang, L. X. Gao, and G. D. Zhou, "Inhibition of copper corrosion in aerated hydrochloric acid solution by heterocyclic compounds containing a mercapto group," *Corrosion Science*, vol. 46, no. 12, pp. 3031–3040, 2004.

[9] F. Bentiss, M. Lagrenee, M. Traisnel, and J. C. Hornez, "The corrosion inhibition of mild steel in acidic media by a new triazole derivative," *Corrosion Science*, vol. 41, no. 4, pp. 789–803, 1999.

[10] E. McCafferty, V. Pravdic, and A. C. Zettlemoyer, "Dielectric behaviour of adsorbed water films on the α-Fe_2O_3 surface," *Transactions of the Faraday Society*, vol. 66, pp. 1720–1731, 1970.

[11] F. Bentiss, M. Lebrini, and M. Lagrenée, "Thermodynamic characterization of metal dissolution and inhibitor adsorption processes in mild steel/2,5-bis(*n*-thienyl)-1,3,4-thiadiazoles/hydrochloric acid system," *Corrosion Science*, vol. 47, no. 12, pp. 2915–2931, 2005.

[12] F. El-Taib Heakal and S. Haruyama, "Impedance studies of the inhibitive effect of benzotriazole on the corrosion of copper in sodium chloride medium," *Corrosion Science*, vol. 20, no. 7, pp. 887–898, 1980.

[13] U. J. Ekpe, U. J. Ibok, B. I. Ita, O. E. Offiong, and E. E. Ebenso, "Inhibitory action of methyl and phenyl thiosemicarbazone derivatives on the corrosion of mild steel in hydrochloric acid," *Materials Chemistry & Physics*, vol. 40, no. 2, pp. 87–93, 1995.

[14] M. Metikos-Hukovic, Z. Grubac, and E. Stupnisek-Lisac, "Organic corrosion inhibitors for aluminum in perchloric acid," *Corrosion*, vol. 50, no. 2, pp. 146–151, 1994.

[15] A. W. Adamson, *Physical Chemistry of Surfaces*, John Wiley & Sons, New York, NY, USA, 1990.

[16] T. Arslan, F. Kandemirli, E. E. Ebenso, I. Love, and H. Alemu, "Quantum chemical studies on the corrosion inhibition of some sulphonamides on mild steel in acidic medium," *Corrosion Science*, vol. 51, no. 1, pp. 35–47, 2009.

[17] E. Jamalizadeh, A. H. Jafari, and S. M. A. Hosseini, "Semi-empirical and ab initio quantum chemical characterisation of pyridine derivatives as HCl inhibitors of aluminium surface," *Journal of Molecular Structure: THEOCHEM*, vol. 870, no. 1–3, pp. 23–30, 2008.

[18] D. Q. Zhang, Q. R. Cai, L. X. Gao, and K. Y. Lee, "Effect of serine, threonine and glutamic acid on the corrosion of copper in aerated hydrochloric acid solution," *Corrosion Science*, vol. 50, no. 12, pp. 3615–3621, 2008.

[19] G. Gece, "The use of quantum chemical methods in corrosion inhibitor studies," *Corrosion Science*, vol. 50, no. 11, pp. 2981–2992, 2008.

[20] G. Gece and S. Bilgiç, "Quantum chemical study of some cyclic nitrogen compounds as corrosion inhibitors of steel in NaCl media," *Corrosion Science*, vol. 51, no. 8, pp. 1876–1878, 2009.

[21] M. Bouklah, B. Hammouti, M. Lagrenée, and F. Bentiss, "Thermodynamic properties of 2,5-bis(4-methoxyphenyl)-1,3,4-oxadiazole as a corrosion inhibitor for mild steel in normal sulfuric acid medium," *Corrosion Science*, vol. 48, no. 9, pp. 2831–2842, 2006.

[22] J. A. Van Allan and B. D. Deagon, *Organic Syntheses Collect*, vol. 4, John Wiley & Sons, New York, NY, USA, 1963.

[23] A. Popova, E. Sokolova, S. Raicheva, and M. Christov, "AC and DC study of the temperature effect on mild steel corrosion in acid media in the presence of benzimidazole derivatives," *Corrosion Science*, vol. 45, no. 1, pp. 33–58, 2003.

[24] M. M. El-Naggar, "Corrosion inhibition of mild steel in acidic medium by some sulfa drugs compounds," *Corrosion Science*, vol. 49, no. 5, pp. 2226–2236, 2007.

[25] Y. Li, P. Zhao, Q. Liang, and B. Hou, "Berberine as a natural source inhibitor for mild steel in 1 M H_2SO_4," *Applied Surface Science*, vol. 252, no. 5, pp. 1245–1253, 2005.

[26] M. Abdallah, "Antibacterial drugs as corrosion inhibitors for corrosion of aluminium in hydrochloric solution," *Corrosion Science*, vol. 46, no. 8, pp. 1981–1996, 2004.

[27] S. A. Umoren and E. E. Ebenso, "The synergistic effect of polyacrylamide and iodide ions on the corrosion inhibition of mild steel in H_2SO_4," *Materials Chemistry and Physics*, vol. 106, no. 2-3, pp. 387–393, 2007.

[28] A. Y. El-Etre, "Inhibition of acid corrosion of aluminum using vanillin," *Corrosion Science*, vol. 43, no. 6, pp. 1031–1039, 2001.

[29] L. Larabi, O. Benali, S. M. Mekelleche, and Y. Harek, "2-Mercapto-1-methylimidazole as corrosioninhibitor for copper in hydrochloric acid," *Applied Surface Science*, vol. 253, no. 3, pp. 1371–1378, 2006.

[30] M. Lebrini, F. Bentiss, H. Vezin, and M. Lagrenée, "The inhibition of mild steel corrosion in acidic solutions by 2,5-bis(4-pyridyl)-1,3,4-thiadiazole: structure-activity correlation," *Corrosion Science*, vol. 48, no. 5, pp. 1279–1291, 2006.

[31] I. B. Obot, N. O. Obi-Egbedi, and S. A. Umoren, "Antifungal drugs as corrosion inhibitors for aluminium in 0.1 M HCl," *Corrosion Science*, vol. 51, no. 8, pp. 1868–1875, 2009.

[32] M. Lebrini, M. Lagrenée, H. Vezin, L. Gengembre, and F. Bentiss, "Electrochemical and quantum chemical studies of new thiadiazole derivatives adsorption on mild steel in normal hydrochloric acid medium," *Corrosion Science*, vol. 47, no. 2, pp. 485–505, 2005.

[33] I. N. Putilova, S. A. Balezin, and V. P. Barannik, *Metallic Corrosion Inhibitors*, Pergamon Press, Elmsford, NY, USA, 1960.

[34] M. A. Elmorsi and A. M. Hassanein, "Corrosion inhibition of copper by heterocyclic compounds," *Corrosion Science*, vol. 41, no. 12, pp. 2337–2352, 1999.

[35] I. Dehri and M. Özcan, "The effect of temperature on the corrosion of mild steel in acidic media in the presence of some sulphur-containing organic compounds," *Materials Chemistry and Physics*, vol. 98, no. 2-3, pp. 316–323, 2006.

[36] G. P. Cicileo, B. M. Rosales, F. E. Varela, and J. R. Vilche, "Comparative study of organic inhibitors of copper corrosion," *Corrosion Science*, vol. 41, no. 7, pp. 1359–1375, 1999.

[37] M. Pourbaix, *Atlas of Electrochemical Equilibria in Aqueous Solutions*, NACE, Houston, Tex, USA, 1975.

[38] H. E. Johnson and J. Leja, "On the Potential/pH-Diagrams of Cu–NH_3–H_2O and Zn–NH_3–H_2O systems," *Journal of the Electrochemical Society*, vol. 112, no. 6, pp. 638–641, 1965.

[39] S. S. Abd El-Rehim, S. A. M. Refaey, F. Taha, M. B. Saleh, and R. A. Ahmed, "Corrosion inhibition of mild steel in acidic medium using 2-amino thiophenol and 2-cyanomethyl benzothiazole," *Journal of Applied Electrochemistry*, vol. 31, no. 4, pp. 429–435, 2001.

[40] H. Ashassi-Sorkhabi, B. Shabani, B. Aligholipour, and D. Seifzadeh, "The effect of some Schiff bases on the corrosion of aluminum in hydrochloric acid solution," *Applied Surface Science*, vol. 252, no. 12, pp. 4039–4047, 2006.

[41] E. E. Ebenso, D. A. Isabirye, and N. O. Eddy, "Adsorption and quantum chemical studies on the inhibition potentials of some thiosemicarbazides for the corrosion of mild steel in acidic medium," *International Journal of Molecular Sciences*, vol. 11, no. 6, pp. 2473–2498, 2010.

[42] M. Hosseini, S. F. L. Mertens, M. Ghorbani, and M. R. Arshadi, "Asymmetrical Schiff bases as inhibitors of mild steel corrosion in sulphuric acid media," *Materials Chemistry and Physics*, vol. 78, no. 3, pp. 800–808, 2003.

[43] Sk. A. Ali, M. T. Saeed, and S. U. Rahman, "The isoxazolidines: a new class of corrosion inhibitors of mild steel in acidic medium," *Corrosion Science*, vol. 45, no. 2, pp. 253–266, 2003.

[44] J. D. Talati and D. K. Gandhi, "N-heterocyclic compounds as corrosion inhibitors for aluminium-copper alloy in hydrochloric acid," *Corrosion Science*, vol. 23, no. 12, pp. 1315–1332, 1983.

[45] Z. Szklarska-Smialowska and J. Mankowski, "Crevice corrosion of stainless steels in sodium chloride solution," *Corrosion Science*, vol. 18, no. 11, pp. 953–960, 1978.

[46] A. Yurt, S. Ulutas, and H. Dal, "Electrochemical and theoretical investigation on the corrosion of aluminium in acidic solution containing some Schiff bases," *Applied Surface Science*, vol. 253, no. 2, pp. 919–925, 2006.

[47] W. Durnie, R. De Marco, A. Jefferson, and B. Kinsella, "Development of a structure-activity relationship for oil field corrosion inhibitors," *Journal of the Electrochemical Society*, vol. 146, no. 5, pp. 1751–1756, 1999.

[48] D. P. Schweinsberg, G. A. George, A. K. Nanayakkara, and D. A. Steinert, "The protective action of epoxy resins and curing agents-inhibitive effects on the aqueous acid corrosion of iron and steel," *Corrosion Science*, vol. 28, no. 1, pp. 33–42, 1988.

[49] A. S. Fouda, M. N. Moussa, F. I. Taha, and A. I. Elneanaa, "The role of some thiosemicarbazide derivatives in the corrosion inhibition of aluminium in hydrochloric acid," *Corrosion Science*, vol. 26, no. 9, pp. 719–726, 1986.

[50] D. Ivanov, *Organic Chemistry*, Nauka i izkustvo, Sofia, Bulgaria, 1964.

[51] Z. Hauptman, U. Graefe, and H. Remane, *Organic Chemistry (Bulg.)*, Nauka i izkustvo, Sofia, Bulgaria, 1985.

[52] S. L. Dyatkina and B. B. Damaskin, "Adsorption behavior of the different forms of dimethylbenzimidazole at the mercury electrode," *Elektrokhimiya*, vol. 22, p. 1283, 1986.

[53] L. Tang, G. Mu, and G. Liu, "The effect of neutral red on the corrosion inhibition of cold rolled steel in 1.0 M hydrochloric acid," *Corrosion Science*, vol. 45, no. 10, pp. 2251–2262, 2003.

[54] D. Q. Zhang, Q. R. Cai, X. M. He, L. X. Gao, and G. S. Kim, "Corrosion inhibition and adsorption behavior of methionine on copper in HCl and synergistic effect of zinc ions," *Materials Chemistry and Physics*, vol. 114, no. 2-3, pp. 612–617, 2009.

[55] N. López and F. Illas, "Ab initio modeling of the metal-support interface: the interaction of Ni, Pd, and Pt on MgO(100)," *Journal of Physical Chemistry B*, vol. 102, no. 8, pp. 1430–1436, 1998.

[56] J. Andrés and J. Beltran, *Química Teórica y Computacional*, Universitat Jaume I, Castellón de la Plana, España, 2000.

[57] M. K. Awad, F. M. Mahgoub, and M. M. El-iskandarani, "Theoretical studies of the effect of structural parameters on the inhibition efficiencies of mercapto-1,2,4-triazoline derivatives," *Journal of Molecular Structure: THEOCHEM*, vol. 531, no. 1–3, pp. 105–117, 2000.

[58] M. K. Awad, "Semiempirical investigation of the inhibition efficiency of thiourea derivatives as corrosion inhibitors," *Journal of Electroanalytical Chemistry*, vol. 567, no. 2, pp. 219–225, 2004.

[59] G. Bereket, C. Öretir, and A. Yurt, "Quantum mechanical calculations on some 4-methyl-5-substituted imidazole derivatives as acidic corrosion inhibitor for zinc," *Journal of Molecular Structure: THEOCHEM*, vol. 571, no. 1–3, pp. 139–145, 2001.

[60] G. Gao and C. Liang, "Electrochemical and DFT studies of β-amino-alcohols as corrosion inhibitors for brass," *Electrochimica Acta*, vol. 52, no. 13, pp. 4554–4559, 2007.

[61] H. Ju, Z. P. Kai, and Y. Li, "Aminic nitrogen-bearing polydentate Schiff base compounds as corrosion inhibitors for iron in acidic media: a quantum chemical calculation," *Corrosion Science*, vol. 50, no. 3, pp. 865–871, 2008.

[62] A. Y. Musa, A. A. H. Kadhum, A. B. Mohamad, A. A. B. Rahoma, and H. Mesmari, "Electrochemical and quantum chemical calculations on 4,4-dimethyloxazolidine-2-thione as inhibitor for mild steel corrosion in hydrochloric acid," *Journal of Molecular Structure*, vol. 969, no. 1–3, pp. 233–237, 2010.

[63] I. B. Obot and N. O. Obi-Egbedi, "Theoretical study of benzimidazole and its derivatives and their potential activity as corrosion inhibitors," *Corrosion Science*, vol. 52, no. 2, pp. 657–660, 2010.

[64] M. Özcan, "AC impedance measurement of cystine adsorption at mild steel/sulfuric acid interface as corrosion inhibitor," *Journal of Solid State Electrochemistry*, vol. 12, no. 12, pp. 1653–1661, 2008.

[65] S. Zor, F. Kandemirli, and M. Bingul, "Inhibition effects of methionine and tyrosine on corrosion of iron in HCl solution: electrochemical, FTIR, and quantum-chemical study," *Protection of Metals and Physical Chemistry of Surfaces*, vol. 45, no. 1, pp. 46–53, 2009.

[66] J. Cruz, T. Pandiyan, and E. García-Ochoa, "A new inhibitor for mild carbon steel: electrochemical and DFT studies," *Journal of Electroanalytical Chemistry*, vol. 583, no. 1, pp. 8–16, 2005.

[67] R. G. Parr, R. A. Donnelly, M. Levy, and W. E. Palke, "Electronegativity: the density functional viewpoint," *The Journal of Chemical Physics*, vol. 68, no. 8, pp. 3801–3807, 1978.

[68] R. G. Parr and R. G. Pearson, "Absolute hardness: companion parameter to absolute electronegativity," *Journal of the American Chemical Society*, vol. 105, no. 26, pp. 7512–7516, 1983.

[69] I. Lukovits, E. Kálmán, and F. Zucchi, "Corrosion inhibitors—correlation between electronic structure and efficiency," *Corrosion*, vol. 57, no. 1, pp. 3–8, 2001.

[70] R. G. Pearson, "Hard and soft acids and bases," *Journal of the American Chemical Society*, vol. 85, no. 22, pp. 3533–3539, 1963.

[71] A. Lesar and I. Milošev, "Density functional study of the corrosion inhibition properties of 1,2,4-triazole and its amino derivatives," *Chemical Physics Letters*, vol. 483, no. 4–6, pp. 198–203, 2009.

[72] P. K. Chattaraj, U. Sarkar, and D. R. Roy, "Electrophilicity index," *Chemical Reviews*, vol. 106, no. 6, pp. 2065–2091, 2006.

[73] B. Gómez, N. V. Likhanova, M. A. Domínguez-Aguilar, R. Martínez-Palou, A. Vela, and J. L. Gázquez, "Quantum chemical study of the inhibitive properties of 2-pyridyl-azoles," *Journal of Physical Chemistry B*, vol. 110, no. 18, pp. 8928–8934, 2006.

[74] J. H. Henríquez-Román, L. Padilla-Campos, M. A. Páez et al., "The influence of aniline and its derivatives on the corrosion behaviour of copper in acid solution: a theoretical approach," *Journal of Molecular Structure: THEOCHEM*, vol. 757, no. 1–3, pp. 1–7, 2005.

[75] H. B. Michaelson, "The work function of the elements and its periodicity," *Journal of Applied Physics*, vol. 48, no. 11, pp. 4729–4733, 1977.

[76] M. J. S. Dewar, E. G. Zoebisch, E. F. Healy, and J. J. P. Stewart, "Development and use of quantum mechanical molecular models. 76. AM1: a new general purpose quantum mechanical molecular model," *Journal of the American Chemical Society*, vol. 107, no. 13, pp. 3902–3909, 1985.

[77] M. K. Awad, M. R. Mustafa, and M. M. Abo Elnga, "Computational simulation of the molecular structure of some triazoles as inhibitors for the corrosion of metal surface," *Journal of Molecular Structure: THEOCHEM*, vol. 959, no. 1–3, pp. 66–74, 2010.

[78] R. G. Pearson, "Absolute electronegativity and hardness: application to inorganic chemistry," *Inorganic Chemistry*, vol. 27, no. 4, pp. 734–740, 1988.

[79] E. C. Koch, "Acid-base interactions in energetic materials—I. The hard and soft acids and bases (HSAB) principle—insights to reactivity and sensitivity of energetic materials," *Propellants, Explosives, Pyrotechnics*, vol. 30, no. 1, pp. 5–16, 2005.

[80] X. Li, S. Deng, H. Fu, and T. Li, "Adsorption and inhibition effect of 6-benzylaminopurine on cold rolled steel in 1.0 M HCl," *Electrochimica Acta*, vol. 54, no. 16, pp. 4089–4098, 2009.

[81] R. Hasanov, M. Sadikoğlu, and S. Bilgiç, "Electrochemical and quantum chemical studies of some Schiff bases on the corrosion of steel in H_2SO_4 solution," *Applied Surface Science*, vol. 253, no. 8, pp. 3913–3921, 2007.

[82] N. Khalil, "Quantum chemical approach of corrosion inhibition," *Electrochimica Acta*, vol. 48, no. 18, pp. 2635–2640, 2003.

[83] M. Lagrenée, B. Mernari, N. Chaibi, M. Traisnel, H. Vezin, and F. Bentiss, "Investigation of the inhibitive effect of substituted oxadiazoles on the corrosion of mild steel in HCl medium," *Corrosion Science*, vol. 43, no. 5, pp. 951–962, 2001.

[84] M. A. Quraishi and R. Sardar, "Hector bases—a new class of heterocyclic corrosion inhibitors for mild steel in acid solutions," *Journal of Applied Electrochemistry*, vol. 33, no. 12, pp. 1163–1168, 2003.

[85] K. F. Khaled, K. Babić-Samardžija, and N. Hackerman, "Theoretical study of the structural effects of polymethylene amines on corrosion inhibition of iron in acid solutions," *Electrochimica Acta*, vol. 50, no. 12, pp. 2515–2520, 2005.

[86] G. Bereket, E. Hür, and C. Öretir, "Quantum chemical studies on some imidazole derivatives as corrosion inhibitors for iron in acidic medium," *Journal of Molecular Structure: THEOCHEM*, vol. 578, no. 1–3, pp. 79–88, 2002.

[87] J. Fang and J. Li, "Quantum chemistry study on the relationship between molecular structure and corrosion inhibition efficiency of amides," *Journal of Molecular Structure: THEOCHEM*, vol. 593, no. 1–3, pp. 179–185, 2002.

[88] H. Ju, Z.-P. Kai, and Y. Li, "Aminic nitrogen-bearing polydentate Schiff base compounds as corrosion inhibitors for iron in acidic media: a quantum chemical calculation," *Corrosion Science*, vol. 50, no. 3, pp. 865–871, 2008.